Combining Anatomic, Metabolic and Physiologic MR Imaging parameters to Distinguish Recurrent High-Grade Glioma from Treatment-Induced Effects

J. Cluceru[1,2], S.J. Nelson[1,2], A.M. Molinaro[3], J.J. Phillips[3], M. P. Olson[1], M. LaFontaine[1], A. Jakary[1], D. Nair[1], S. Cha[1], S.M. Chang[3], J.M. Lupo[1]

[1]Dept. Radiology & Biomedical Imaging, [2]Dept. Bioengineering and Therapeutic Sciences, [3]Dept. Neurological Surgery

Overview

MOTIVATION

- Damage induced by chemotherapy and radiation mimics high grade glioma recurrence [1] (Figure 1).
- Radiologists cannot distinguish between these two phenomena and therefore physiologic and metabolic MRI should be used to probe underlying biological difference between treatment induced effects (TxE) and true recurrent high grade glioma (rHGG).
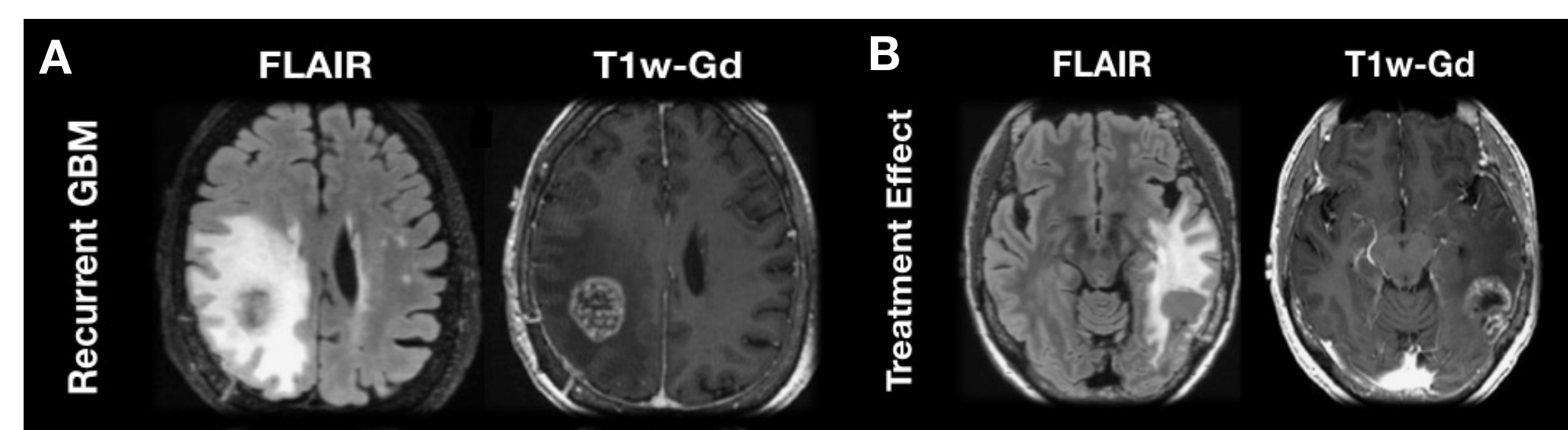- Distinguishing TxE from rHGG has great implications for treatment planning and clinical trial endpoint evaluation.

Figure 1. Visual comparison of recurrent HGG and treatment-induced effects. (A) Representative FLAIR and T1w-Gd contrast enhanced (CE) from a recurrent GBM. (B) Representative TMZ and RT induced effects for a suspected recurrent HGG, confirmed TxE from histopathological analysis after resection.

THE ROLE OF PHYSIOLOGIC & METABOLIC MRI

- Diffusion weighted imaging (DWI) & diffusion tensor imaging (DTI): ↑ cellularity proliferative tumor potentiates restricted water diffusion, more so than ↑ cellularity from treatment-induced inflammation (Figure 3) [1]; *Parameters used*: ADC = apparent diffusion coeff; FA = fractional anisotropy
- Dynamic susceptibility contrast perfusion-weighted imaging (DSC): Rapid tumor cell division potentiates ↑ angiogenesis and ↑ blood-brain barrier (BBB) breakdown (Figure 4) [4]; *Parameters used:* CBV = cerebral blood volume, PH = deltaR2* peak height, RECOV = percent deltaR2* signal recovery.
- Magnetic resonance spectroscopic imaging (MRSI): Concentrations of metabolites change wrt disease state; use the metabolism of cancer cells to probe differences among TxE and rHGG; *Parameters used:* nCho, nCre, nLac, nLip, nNAA, CNI: Cho-to-NAA index, [2] CCRI: Cho-to-Cre index (Figure 5)

Methods

Patients/Samples: A total of 393 samples from 148 patients with an original diagnosis of high-grade glioma were included in this study. Each patient was recruited prior to resection. The max number of patients were included per analysis (diffusion: 143 pts, 373 samples; perfusion: 132 pts, 232 samples; spectroscopy: 87 pts 187 samples)

Pathology Outcomes: Tumor score (TS) (pathologist evaluation 0-3, 0 = no tumor, 1= <10% tumor, 2 = 10-50% tumor, 3 = >50% tumor); TS 0&1 vs TS 2&3 (grouped); Mib (Ki-67) proliferation marker; TxE vs rHGG (Figure 2); Necrosis (0-2), Treatment-related abnormal blood vessels.
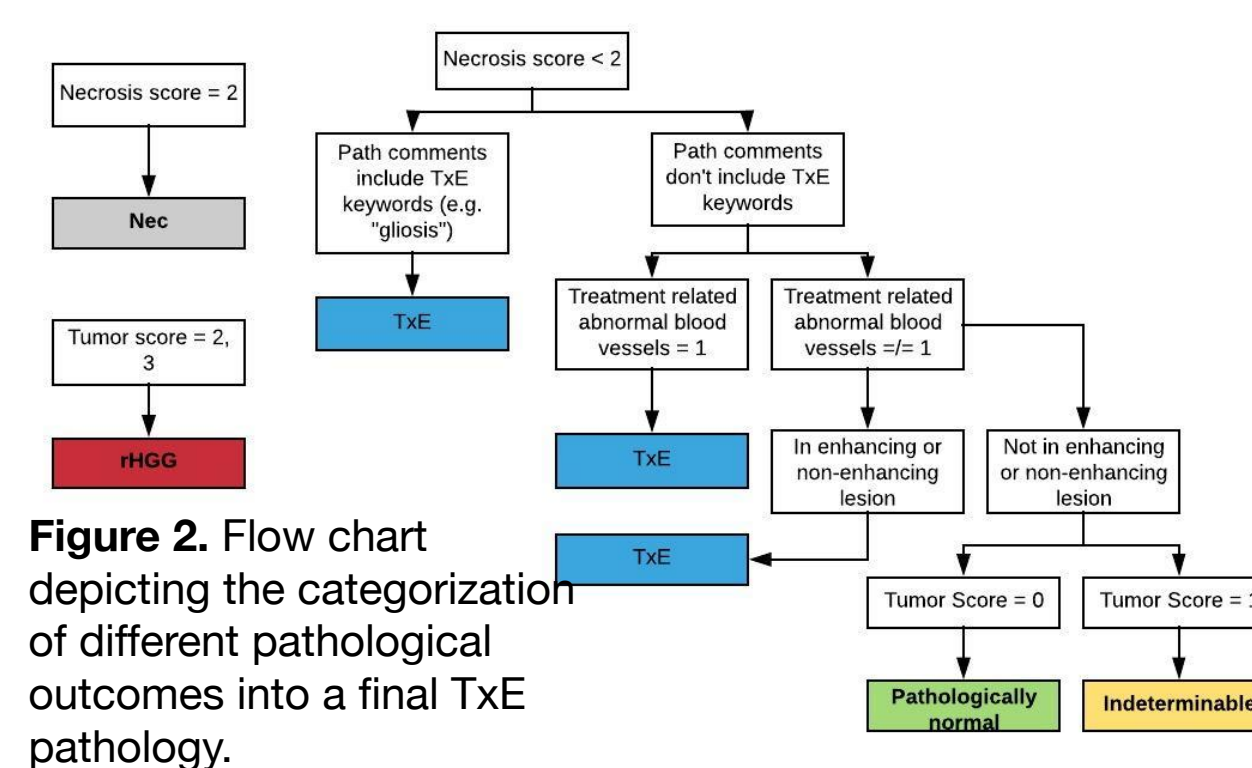

Figure 2. Flow chart depicting the categorization of different pathological outcomes into a final TxE pathology.

Image Acquisition: Patients were scanned on a 3T GE scanner with an 8-channel head coil. *Anatomic:* T2-weighted FLAIR and FSE as well as T1-weighted pre- and post-gadolinium contrast images. *DTI:* SE EPI images, 24directions, b=1000s/mm², 1.7x1.7x3mm resolution *DSC perfusion-weighted imaging*: T2*-weighted EPI images (TR/TE/flip angle = 1250–1500/35–54ms/30–35degrees, 60–80 time points) *3D MRSI:* PRESS volume localization and VSS pulses for lipid signal suppression (TR/TE =1104/144ms, FOV=16×16×16cm³, nominal voxel size=1×1×1cm³).

Statistical Analyses:

- Boxplots and histograms were created to observe differences among the distribution of parameters when binned by outcome
- To assess significance in the association of different parameter changes with outcome, Generalized Estimating Equations, Generalized Linear Mixed Models, and repeated measures ANOVA were used to account for the potential correlation among biopsies derived from the same patient.
- GLMM: $\log\left(\frac{P(Y_{ij}=1)}{P(Y_{ij}=0)}\right) = \beta_0 + \beta_1 x_{ij} + b_i; i = 1 \ldots ns, j = 1 \ldots m$
- GEE: $\log\left(\frac{P(Y_{ij}=1)}{P(Y_{ij}=0)}\right) = \beta_0 + \beta_1 x_{ij}; i = 1 \ldots n, j = 1 \ldots m$
- These binary methods were extended for ordinal and continuous outcomes using `multgee` and `lme4`, and repeated measures ANOVA, whose model can be written as:
- RM ANOVA: $Yij = \gamma_i + \pi_{ji} + \varepsilon ij; i = 1 \ldots n, j = 1 .. m$
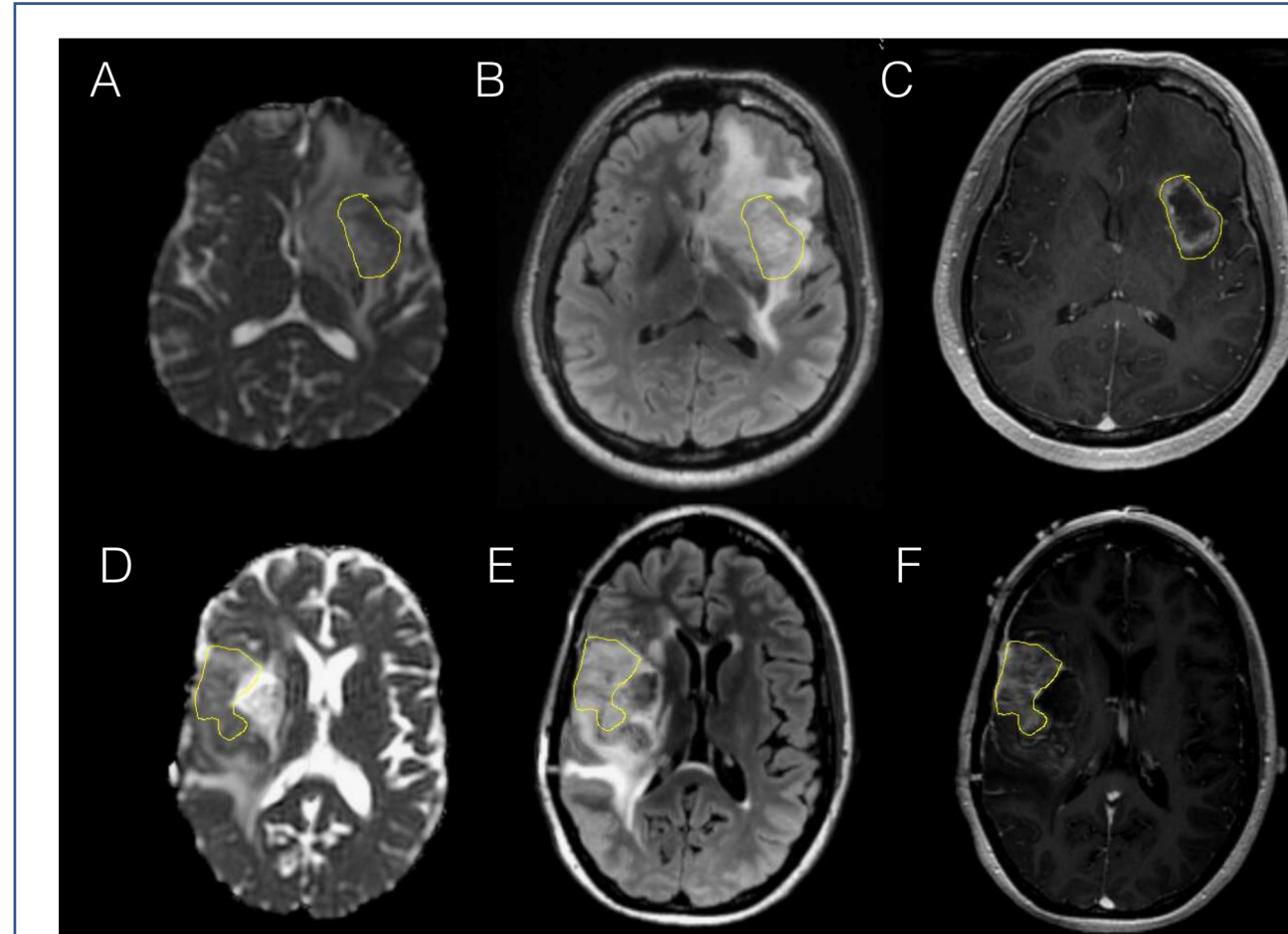- All analyses were completed in R statistical computing language

Figure 3. Comparison of ADC images from DTI among treatment effect (A-C) and true recurrent HGG (D-F). Yellow lines delineate the contrast enhanced (CE) ROIs. ADC in TxE (A) shows minimal decrease near CE, whereas ADC in rHGG shows significant decrease relative to (A). T2w FLAIR images (B, E) depict hyper-intense regions around the CE from T1. T1w gadolinium injected images (C-F) depict regions of CE.
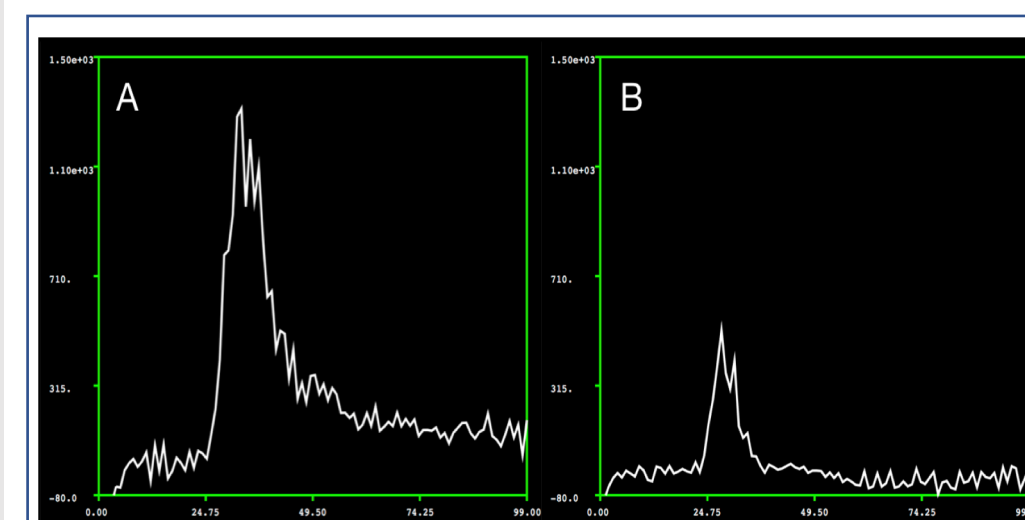

Figure 4. DSC perfusion curve comparison from rHGG vs TxE. Curves representing non-parametric and nonlinear gamma-variate fitting taken from biopsies from (A) pathologically confirmed high-grade glioma and (B) pathologically confirmed treatment effect. Difference in peak height and CBV highlights the utility of DSC imaging in TxE vs. GBM.
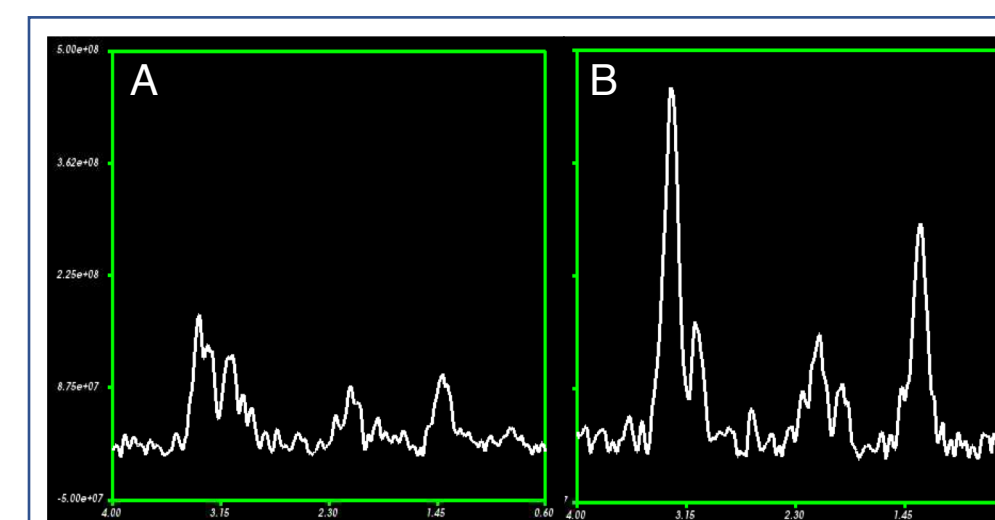

Figure 5. Spectra comparison from rHGG vs TxE. (A) Spectra from a representative voxel taken from a patient experiencing only TxE. (B) Spectra obtained from a representative voxel taken from a patient experiencing recurrent HGG. Spectra shows elevated levels of choline, lactate as compared with (A).

Results

Visual parameter associations: In order to visually assess the differences in the distributions of the parameters calculated from biopsy masks, scatter plots and box plots were created to ensure that parameter behaviour coincided with previous literature. CNI, PH and CBV were consistently elevated in higher grade samples.

Statistical comparison: To confirm visual findings, statistical analyses that account for multiple samples per patient were used. In nearly all tests regardless of outcome, spectroscopy parameter CNI and perfusion parameters CBV and PH were significant.
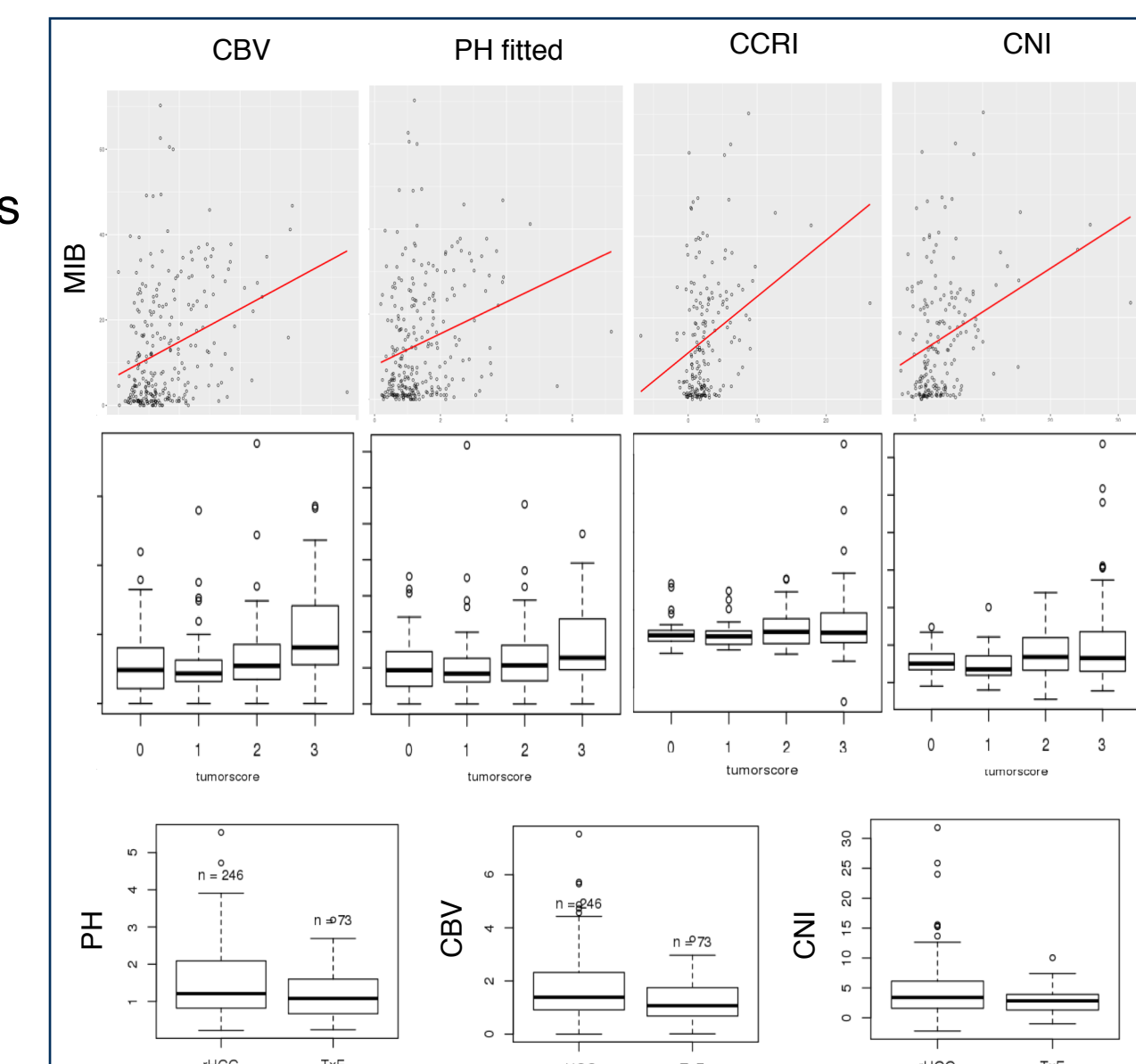

Figure 6. Visual comparisons of highly significant parameters using MIB, tumor score, and TxE vs rHGG outcomes.

MODALITY	PARAMETER	Tumor Score (TS) GEE	Tumor Score (TS) GLMM	TS 0 & 1 vs TS 2 & 3 GEE	TS 0 & 1 vs TS 2 & 3 GLMM	TxE vs rHGG GEE	Ki-67 LMM	Ki-67 RMANOVA
ANATOMIC	T2 FSE INTENSITY	n.s.	n.s.	n.s.	n.s.	n.s.	n.s.	✔
	T2 FLAIR INTENSITY	n.s.	n.s./✔/n.s.	n.s.	✔	n.s.	n.s.	✔
	T1 PRE-CONTRAST INTENSITY	✔	n.s./✔/✔	✔	n.s.	✔	n.s.	✔
	T1 POST-CONTRAST INTENSITY	n.s.	n.s.	n.s.	n.s.	n.s.	n.s.	n.s.
DIFFUSION	APPARENT DIFFUSION COEFF	n.s.	n.s.	n.s.	n.s.	n.s.	n.s.	✔
	FRACTIONAL ANISOTROPY	n.s.	n.s.	n.s.	n.s.	n.s.	n.s.	✔
	FIRST EIGENVALUE	n.s.	n.s.	n.s.	n.s.	n.s.	n.s.	n.s.
	RADIAL EIGENVALUE	n.s.	n.s.	n.s.	n.s.	n.s.	n.s.	n.s.
PERFUSION	PEAK HEIGHT NON-PARAMETRIC	n.s.	n.s./n.s./✔	n.s.	n.s.	✔	✔	✔
	PEAK HEIGHT FITTED	n.s.	n.s./n.s./✔	✔	n.s.	✔	✔	✔
	CEREBRAL BLOOD VOLUME	n.s.	n.s./✔/✔	✔	n.s.	✔	✔	✔
	PERCENT RECOVERY	✔	✔/✔/✔	✔	n.s.	✔	n.s.	✔
SPECTROSCOPY	CHOLINE	n.r.	n.s./n.s./✔	✔	n.s.	✔	n.s.	✔
	CHOLINE-TO-NAA INDEX	n.r.	n.s./n.s./✔	✔	✔	✔	✔	✔
	CHOLINE-TO-CREATINE INDEX	n.r.	n.s.	n.s.	n.s.	✔	n.s.	✔
	CREATINE-TO-NAA INDEX	n.r.	n.s.	✔	n.s.	n.s.	✔	✔
	N-ASPARTYL ACETATE	n.r.	n.s.	n.s.	n.s.	n.s.	n.s.	n.s.
	CREATINE	n.r.	n.s.	n.s.	n.s.	n.s.	n.s.	n.s.
	LIPID+LACTATE	n.r.	n.s.	n.s.	n.s.	n.s.	n.s.	n.s.

Table 1. Results from univariate analysis that show consistent significance for perfusion and spectroscopy parameters including cerebral blood volume, choline-to-naa index, peak height, and normalized choline.

✔	p<.001
✔	p<.01
✔	p<.05

Summary

- This preliminary investigation highlights the recreation of literature findings in gross anatomical ROIs in biopsy-level data.
- Our results suggest that combining nPH or nCBV from DSC-perfusion with CNI from MRSI hold the most promise in identifying regions of recurrent tumor after treatment.
- Future work will apply machine learning techniques to this data.

References

[1] Verma N. et al. *Neuro Oncol* 2013 [2] McKnight TR et al. *J Neurosurg* 2002. [3] Halekoh UJ. et al. *Stat Softw* 2006 [4] Barajas RF et al. *Radiology*, 2009 [5] Jena et al. *American Journal of Neuroradiology*, 2017 [6] Hu LS. et al. *PLoS One* 2015.